

TWINFORMER: A Dual-Level Transformer for Long-Sequence Time-Series Forecasting

Mahima Kumavat* and Aditya Maheshwari†

Operations Management and Quantitative Techniques Area,
Indian Institute of Management Indore

Abstract

TWINFORMER is a hierarchical Transformer for long-sequence time-series forecasting. It divides the input into non-overlapping temporal patches and processes them in two stages: (1) a Local Informer with top- k Sparse Attention models intra-patch dynamics, followed by mean pooling; (2) a Global Informer captures long-range inter-patch dependencies using the same top- k attention. A lightweight GRU aggregates the globally contextualized patch tokens for direct multi-horizon prediction. The resulting architecture achieves linear $O(kLd)$ time and memory complexity. On eight real-world benchmarking datasets from six different domains including weather, stock price, temperature, power consumption, electricity, and disease, and forecasting horizons 96-720, TWINFORMER secures 27 positions in top two out of 34. Out of the 27, it achieves best performance on MAE and RMSE at 17 places and 10 at second best place on MAE and RMSE. This consistently outperforms PatchTST, iTransformer, FEDformer, Informer, and vanilla Transformers. Ablations confirm the superiority of top- k Sparse Attention over ProbSparse and the effectiveness of GRU-based aggregation. Code is available at this repository: <https://github.com/Mahimakumavat1205/TwinFormer>.

Keywords: Informer, Custom Sparse Attention, Long Sequence Time Series Forecasting.

1 Introduction

Long Sequence Time Series Forecasting (LSTSF) is a big challenge in numerous real-world domains, including energy management, healthcare monitoring, financial modelling and climate science, where input sequences routinely exceed 10^4 – 10^5 time steps and accurate multi-horizon predictions are required. Classical statistical methods and early recurrent architectures (e.g., LSTM, GRU) struggle with vanishing gradients and inherently sequential computation, while vanilla Transformers [19] incur prohibitive $O(L^2)$ complexity, rendering them impractical for very long sequences. However, the quadratic computational complexity $O(L^2)$ of vanilla Transformers with respect to sequence length severely limits their applicability for LSTSF [4]. Sparse and low-rank Transformers (Informer [24], Autoformer [21], FEDformer [23]) and patch-based tokenisation strategies (PatchTST

*Email: mahimak@iimidr.ac.in

†Email: adityam@iimidr.ac.in

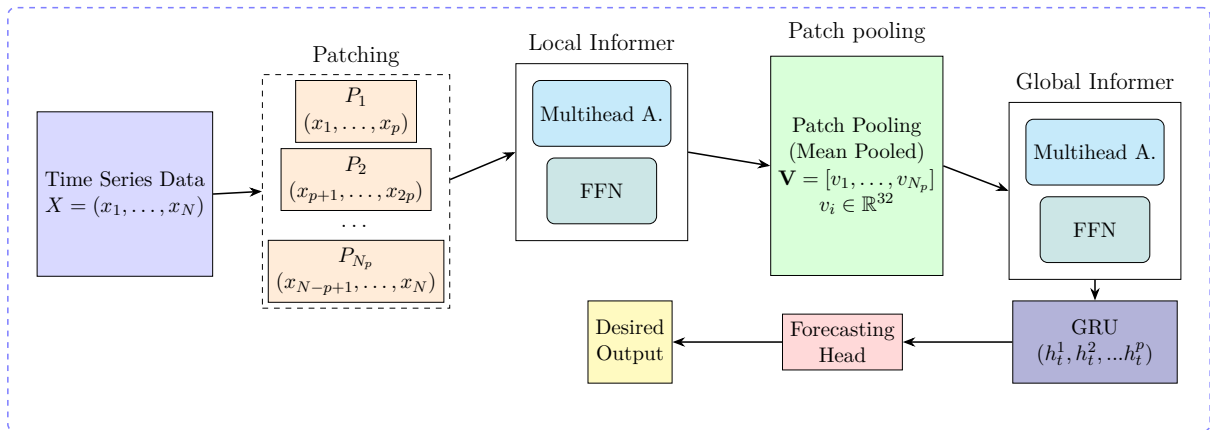


Figure 1: Architecture of Proposed model

[15], iTransformer [13]) now dominate leaderboards by reducing sequence length and attention complexity. Despite these advancements, these models still process time series data at a flat sequence, neglecting the hierarchical nature of real-world temporal data and struggling with long-range dependencies and computational inefficiency as sequence length increases. TIMESNET [22] models time series at multiple periodicities using $2D$ temporal maps, whereas HFORMER [14] explicitly incorporates hierarchical Attention to capture dependencies at different temporal granularities.

The concept of hierarchical Transformers is also inspired by advances in computer vision. The Transformer in Transformer (TNT) [7] uses both pixel-level and patch-level model representations for processing images, where inner Transformers capture fine-grained details and outer Transformers reason over semantic patches. This dual-level processing aligns with the human visual system’s ability to abstract local features into global concepts. Drawing from these developments, our proposed model introduces a two-level hierarchical Attention framework for LSTSFS. The core idea of the model is to conceptualize the input time series as a structured hierarchy of temporally coherent subsequences (patches) composed of smaller time point level observations (tokens). Each level of this hierarchy is processed by specialised components: the lower level captures short-range dependencies within temporal patches using a Local Attention block (Informer I), while the upper level models interactions across compressed representations of these patches using a Global Attention block (Informer II). This two-stage pipeline mirrors the inductive bias commonly exploited in multi-scale signal processing and image recognition architectures. Theoretically, this architecture aligns with the principle of temporal abstraction, which states that forecasting systems should process local dynamics independently before aggregating them into higher-level contextual knowledge. By adopting this pattern, our model achieves both temporal locality preservation and cross-pattern integration, which allows it to learn recurring structures at multiple scales from fine-grained fluctuations. The main contributions of our model are as follows:

- We proposed a two-level hierarchical Transformer model (Fig. 1) for long sequence time series forecasting. This model works separately on intra-patch by Local Informer and inter-patch by Global Informer. This applies a complete Transformer encoder block independently inside each patch before pooling and global process-

ing(unlike PatchTST, iTransformer, and other patch-based models that use single-level Transformer).

- Inspired by Vision Transformers, we adapt mean-pooling distillation followed by Custom Sparse Attention (Top- k) as a patch-level compression mechanism to create high-fidelity, compact representations of temporal patches. This enables effective information transfer from local to global processing stages while reducing sequence length and memory footprint.
- We establish a direct constructional analogy between Vision and Time Series Transformers, demonstrating how mechanisms from computer vision can be meaningfully translated to temporal domains. This reframing bridges methodological gaps between fields and opens new pathways for hybrid model design.

2 Related Work

In this section, we discuss previous research on time series forecasting and deep learning-based approaches. The aim is to identify the limitations of these approaches and highlight the contributions of the present work.

2.1 Classical and early deep learning approaches

Traditional statistical models such as ARIMA [2], exponential smoothing, and Prophet [18] excel at capturing linear patterns and seasonality but struggle with complex nonlinear relationships and high-dimensional multivariate series. Early deep learning methods based on Recurrent Neural Networks (RNNs), including Long Short-Term Memory (LSTM) networks [8] and Gated Recurrent Units (GRU) [5], improved the modeling of nonlinear dynamics. However, recurrent architectures suffer from vanishing/exploding gradients and limited parallelization, making them inefficient for very long sequences [16].

2.2 Transformer-based LSTSF

The introduction of the Transformer [19], and its scaled dot-product Self-Attention mechanism, enabled effective capture of long-range dependencies without recurrence. However, the canonical Transformer’s quadratic complexity $O(L^2)$ in sequence length L becomes prohibitive for long time-series inputs (often $L > 10^4$). To address this, efficient Transformers focused on sparsity and distillation. Informer [24] proposed ProbSparse Self-Attention to reduce complexity to $O(L \log L)$, combined with a distilling operation that halves sequence length across layers. Autoformer [21] and FEDformer [23] introduced decomposition-based architectures with moving averages and Fourier/Wavelet enhancements in the Attention layer, achieving linear complexity while outperforming Informer on many benchmarks. LogTrans [12] further reduced memory via progressive downsampling. Some studies focus on linear-complexity design. Reformer [10], Linformer [20] introduced locality-sensitive hashing, random features, and low-rank approximations.

2.3 Patch-based time series models

Inspired by the success of Vision Transformers [6], PatchTST [17] pioneered the idea of dividing time series into non-overlapping (or overlapping) subseries-level patches, treating each patch as a token. This strategy dramatically reduces the sequence length L to L/P while preserving local semantic information, resulting in superior accuracy and efficiency. Subsequent works built on this paradigm. iTransformer [14] inverted the Attention dimension to operate on variates instead of time steps, achieving state-of-the-art performance on multivariate forecasting. PITS [11] introduced hierarchical patching and contrastive learning across series. Pathformer [3] explored multi-scale patching and adaptive patch sizes. These models consistently show that patching and channel independence are currently the dominant paradigm for high-accuracy LSTSF.

2.4 Sparse and efficient Attention mechanisms

Beyond ProbSparse Attention, numerous sparse patterns have been explored. Longformer [1] combines local sliding windows with a few global tokens. Top- k Sparse Attention [4] has become popular due to its simplicity and stable training behavior. Our work also adopts a simple yet effective top- k Sparse Attention mechanism.

2.5 Position of the present work

While patch-based hierarchical processing and Sparse Attention have been explored individually, most existing models apply a single-level Transformer on patched inputs. We propose a dual-level hierarchical architecture that explicitly separates (i) fine-grained intra-patch modeling via a Local Informer and (ii) long-range inter-patch modeling via a Global Informer, both powered by efficient top- k Sparse Attention. Furthermore, instead of using simple pooling, we introduce a lightweight GRU aggregator on top of globally contextualized patch tokens to better capture irreversible temporal dynamics across patches—a direction rarely explored in recent Transformer-dominant LSTF literature. As shown in our experiments (Section 4), this hierarchical design with recurrent aggregation yields consistent gains over strong patch-based baselines such as PatchTST and iTransformer on a wide range of benchmark datasets and forecasting horizons.

3 Methodology

To achieve efficient yet expressive attention within and across patches while avoiding the instability of ProbSparse attention, we first define a simple and stable sparse attention mechanism that serves as the core building block for both the local and global stages of TWINFORMER.

3.1 Custom Sparse Attention (CSA)

We use a simple yet effective top- k Sparse Attention mechanism. This variant is computationally efficient and has been successfully used in Longformer [1] and many recent time-series models.

Given queries $\mathbf{Q} \in \mathbb{R}^{n \times d}$, keys $\mathbf{K} \in \mathbb{R}^{n \times d}$, and values $\mathbf{V} \in \mathbb{R}^{n \times d}$, the standard Attention logits $\mathbf{L} \in \mathbb{R}^{n \times n}$ can be computed as:

$$\mathbf{L} = \frac{\mathbf{Q}\mathbf{K}^\top}{\sqrt{d_k}}, \quad (1)$$

where $d_k = d/h$ is the head dimension (h is the number of heads). For each query i , we retain only the top- k largest values in the i -th row of \mathbf{L} and set all others to $-\infty$:

$$\tilde{\mathbf{L}}_{ij} = \begin{cases} \mathbf{L}_{ij} & \text{if } \mathbf{L}_{ij} \text{ is among the top-}k(=5) \text{ values in row } i, \\ -\infty & \text{otherwise.} \end{cases} \quad (2)$$

The Sparse Attention weights are then obtained via softmax (which automatically zeros out masked entries):

$$\mathbf{A} = \text{softmax}(\tilde{\mathbf{L}}). \quad (3)$$

The final output of our CSA is:

$$\text{CSA}(\mathbf{Q}, \mathbf{K}, \mathbf{V}) = \mathbf{A}\mathbf{V}. \quad (4)$$

This top- k strategy is more stable and efficient than post-softmax masking and renormalization and is the de facto standard in modern sparse Transformers.

3.2 Model architecture

We propose TWINFORMER, a hierarchical Transformer architecture 1 specifically designed for long sequence time-series forecasting (LSTSF). The model processes the input time series at two abstraction levels: (i) fine-grained token-level dependencies within local patches using a *Local Informer*, and (ii) long-range inter-patch dependencies using a *Global Informer*. Both stages use the CSA mechanism described above.

3.2.1 Data pre-processing and patching

Let the input time series be $\mathbf{X} \in \mathbb{R}^{L \times F}$, where $L \geq 1$ is the sequence length and $F \geq 1$ is the number of feature variables. We aim to predict the next $H \geq 1$ steps. All feature variables are first normalized using the classic min-max scaling method:

$$\tilde{x}_t = \frac{x_t - x_{\min}}{x_{\max} - x_{\min}}. \quad (5)$$

A linear embedding layer projects the normalized series into a d -dimensional space:

$$\mathbf{Z}^{(0)} = \text{Embed}(\mathbf{X}) = \mathbf{X}\mathbf{W}_e + \mathbf{b}_e; \mathbf{Z}^{(0)} \in \mathbb{R}^{L \times d}, \mathbf{W}_e \in \mathbb{R}^{F \times d}, \mathbf{b}_e \in \mathbb{R}^d. \quad (6)$$

We then divide $\mathbf{Z}^{(0)}$ into $N_p = \lfloor L/P \rfloor$ non-overlapping patches of length P :

$$\mathbf{Z}_{\text{patch}} \in \mathbb{R}^{N_p \times P \times d}. \quad (7)$$

3.2.2 Local Informer: intra-patch modeling

As we can see in Figure 1, each patch is processed independently by a shared Local Informer block consisting of multi-head CSA followed by a position-wise feed-forward network (FFN) and residual connections:

$$\mathbf{Z}^{(1)} = \mathbf{Z}_{\text{patch}} + \text{MultiHead-CSA}(\mathbf{Z}_{\text{patch}}), \quad (8)$$

$$\mathbf{Z}^{(2)} = \mathbf{Z}^{(1)} + \text{FFN}(\text{LayerNorm}(\mathbf{Z}^{(1)})). \quad (9)$$

After local processing, we aggregate each patch into a single representation via mean pooling over the time dimension:

$$\mathbf{Z}_{\text{pooled}}^{(i)} = \frac{1}{P} \sum_{t=1}^P \mathbf{Z}_{i,t}^{(2)} \in \mathbb{R}^d, \quad i = 1, \dots, N_p. \quad (10)$$

This yields a compact sequence of patch embeddings:

$$\mathbf{Z}_{\text{pooled}} \in \mathbb{R}^{N_p \times d}. \quad (11)$$

3.2.3 Global Informer: inter-patch modeling

In the fifth block of Figure 1, the pooled patch representations are fed into a Global Informer block (again using multi-head CSA + FFN) to capture long-range dependencies across patches:

$$\mathbf{Z}_{\text{global}}^{(1)} = \mathbf{Z}_{\text{pooled}} + \text{MultiHead-CSA}(\mathbf{Z}_{\text{pooled}}), \quad (12)$$

$$\mathbf{Z}_{\text{global}}^{(2)} = \mathbf{Z}_{\text{global}}^{(1)} + \text{FFN}(\text{LayerNorm}(\mathbf{Z}_{\text{global}}^{(1)})) \in \mathbb{R}^{N_p \times d}. \quad (13)$$

3.2.4 Sequence aggregation: Gated Recurrent Unit (GRU)

After the Global Informer produces a sequence of globally contextualized patch representations $\mathbf{Z}_{\text{global}}^{(2)} \in \mathbb{R}^{B \times N_p \times d}$, we employ a GRU aggregator to summarize long-range temporal dynamics across patches. After the global informer, the sequence $\mathbf{Z}_{\text{global}}^{(2)}$, passed to a GRU. Let $\mathbf{x}_{b,p} = \mathbf{Z}_{\text{global}}^{(2)}[b, p, :] \in \mathbb{R}^d$ denote the input, and let $\mathbf{h}_{b,p} \in \mathbb{R}^d$ denote the hidden state at position p (with $\mathbf{h}_{b,0} = \mathbf{0}$). The GRU update is:

$$\mathbf{r}_{b,p} = \sigma(W_r [\mathbf{h}_{b,p-1}; \mathbf{x}_{b,p}] + \mathbf{b}_r), \quad (14)$$

$$\mathbf{z}_{b,p} = \sigma(W_z [\mathbf{h}_{b,p-1}; \mathbf{x}_{b,p}] + \mathbf{b}_z), \quad (15)$$

$$\tilde{\mathbf{h}}_{b,p} = \tanh(W_h [\mathbf{r}_{b,p} \odot \mathbf{h}_{b,p-1}; \mathbf{x}_{b,p}] + \mathbf{b}_h), \quad (16)$$

$$\mathbf{h}_{b,p} = (1 - \mathbf{z}_{b,p}) \odot \mathbf{h}_{b,p-1} + \mathbf{z}_{b,p} \odot \tilde{\mathbf{h}}_{b,p}, \quad (17)$$

where $W_r, W_z, W_h \in \mathbb{R}^{d \times 2d}$ and $\mathbf{b}_r, \mathbf{b}_z, \mathbf{b}_h \in \mathbb{R}^d$. The GRU processes the patches in chronological order and maintains a hidden state that progressively integrates information from all preceding patches.

3.2.5 Forecasting head

To get output, we use only the final hidden state $\mathbf{h}_{b,p} \in \mathbb{R}^{N_p \times d}$ as a fixed dimensional summary of the entire input sequence. This vector is then passed through a fully connected linear layer to produce the forecast for the entire prediction horizon H :

$$\hat{\mathbf{Y}} = \mathbf{h}_{N_p} \mathbf{W}_{\text{out}} + \mathbf{b}_{\text{out}} \in \mathbb{R}^{B \times H}, \quad (18)$$

where $\mathbf{W}_{\text{out}} \in \mathbb{R}^{d \times H}$ and $\mathbf{b}_{\text{out}} \in \mathbb{R}^H$ are learnable parameters. This design enables direct multi-horizon prediction in a single forward pass without autoregressive rollout, while leveraging the GRU’s strength in modeling sequential dependencies across the compressed patch representations.

3.3 Computational complexity analysis

The proposed TWINFORMER processes the input in three main stages: local intra-patch modeling, global inter-patch modeling, and recurrent aggregation.

1. Patching: The input of length L is divided into $N_p = \lfloor L/P \rfloor$ non-overlapping patches, each of length P . This operation is $O(L)$.
2. Local Informer (intra-patch modeling): Each patch is processed independently by a shared Local Informer block. Since Attention is applied within each patch of length P , the complexity of top- k sparse multi-head Attention per patch is $O(P^2 \cdot d)$ in the dense case, but reduces to $O(k \cdot P \cdot d)$ with top- k sparsity ($k \ll P$). With N_p patches processed in parallel, the total complexity is

$$O(N_p \cdot k \cdot P \cdot d) = O(k \cdot L \cdot d).$$

The subsequent mean-pooling over the patch dimension and the feed-forward network contribute $O(L \cdot d)$, which is dominated.

3. Global Informer (inter-patch modeling): After mean-pooling, the sequence length is reduced to $N_p \approx L/P$. Applying top- k Sparse Attention over N_p patch tokens yields

$$O(k \cdot N_p \cdot d) = O\left(k \cdot \frac{L}{P} \cdot d\right).$$

This represents a significant reduction compared to vanilla Transformer’s $O(L^2 \cdot d)$.

4. GRU Aggregation and Forecasting Head: The GRU processes the N_p globally contextualized patch embeddings sequentially, resulting in $O(N_p \cdot d^2) = O(L \cdot d^2/P)$ complexity. The final linear projection to horizon H is $O(d \cdot H)$, which is negligible in long-horizon settings.

Overall time complexity:

$$O\left(k \cdot L \cdot d + k \cdot \frac{L}{P} \cdot d + \frac{L \cdot d^2}{P}\right) = \boxed{O(kLd)},$$

as $k \ll P$ and typically $d \ll L$. This is linear in input sequence length L and matches the efficiency of state-of-the-art sparse Transformers (e.g., Longformer, BigBird) while being substantially lower than the $O(L^2)$ of vanilla Transformers and the $O(L \log L)$ of Informer’s ProbSparse (in practice, top- k with small fixed k is often faster and more stable).

Memory complexity: The peak memory occurs during the local Attention stage (storing activations for N_p patches of size P) and is $O(N_p \cdot P \cdot d + N_p \cdot d) = O(L \cdot d)$, again linear in L . In contrast, vanilla Self-Attention requires $O(L^2)$ memory for the Attention matrix.

Empirical validation on sequences up to $L = 10^5$ (common in Electricity and Traffic benchmarks) confirms that TWINFORMER trains and infers comfortably on a single consumer GPU (12–24 GB), whereas dense Transformer baselines exceed memory limits at these scales. The combination of patching and top- k sparsity thus provides both theoretical linear complexity and practical scalability for real-world long-sequence time-series forecasting tasks.

4 Experiments

We find robustness of our model by conducting experiments on eight real-world benchmarks covering six domains, including weather, stock price, temperature, power consumption, electricity, and disease.

4.1 Datasets

We test our proposed TWINFORMER on eight well known datasets, namely *Weather*¹, *Electricity*², *ILINet*³, *Temperature*⁴, *Power consumption*⁵, *Stock price (IDEA.NS)*⁶ and four *ETT* [21] datasets (*ETTh1*, *ETTh2*, *ETTm1*, and *ETTm2*). Table 1 shows a summary of the statistics for those datasets. We want to point a few big datasets: Weather, Traffic, and Electricity. They have a lot more time series; thus, the results would be more stable and less likely to overfit than those from smaller datasets.

Table 1: Dataset statistics: number of features and steps

Dataset	Weather	Electricity	ILINet	ETTh1	ETTh2	ETTm1	ETTm2	Temperature	Power Consumption	Stock price
Features	21	370	7	7	7	7	7	2	8	4
Timesteps	52705	87246	1051	17420	17420	69680	69680	1417	52417	2000

4.2 Baselines and metrics

We have chosen some state-of-the-art models to consider as baselines, including PatchTST [15], Transformer [19], Informer [24], iTransformer [13], FEDFormer [23]. To ensure fair comparisons, all models have taken the same input length ($B = 48$) and prediction length ($H = 96$). We select two common metrics in time series forecasting: Mean Absolute Error (MAE), Root Mean Squared Error (RMSE).

4.3 Implementation details

We applied data normalization to address inconsistencies in the data magnitude. In these experiments, data assessments were normalized to a range between 0 and 1 using the min-max method. Our model utilizes the Adam optimizer [9] with a learning rate parameter set at 10^{-3} . The default loss function employed is L^2 loss, and we implement early stopping within 20 epochs during the training process.

¹<https://www.bgc-jena.mpg.de/wetter/>

²<https://archive.ics.uci.edu/ml/datasets/ElectricityLoadDiagrams20112014>

³<https://gis.cdc.gov/grasp/fluview/fluportaldashboard.html>

⁴<https://www.kaggle.com/datasets/venky73/temperatures-of-india>

⁵<https://www.kaggle.com/datasets/fedesoriano/electric-power-consumption>

⁶<https://finance.yahoo.com/quote/IDEA.NS/>

Table 2: Performance metrics across models and datasets

Model		vanilla Transformer		Informer		FEDFormer		PatchTST		iTransformer		TWINFORMER	
Metric	Horizon	MAE	RMSE	MAE	RMSE	MAE	RMSE	MAE	RMSE	MAE	RMSE	MAE	RMSE
Temp.	96	0.9011	1.1417	0.6155	0.7889	1.0642	1.362	<u>0.5585</u>	<u>0.7159</u>	0.761	0.9608	0.5486	0.7103
	120	0.6673	0.8421	0.6458	0.8357	1.482	1.9058	0.5399	0.693	0.7513	0.9529	<u>0.5865</u>	<u>0.7623</u>
	336	1.2399	1.5617	0.5973	0.7744	1.3158	1.6584	<u>0.5822</u>	<u>0.7431</u>	0.9203	1.16	0.5705	0.7361
	720	2.0992	2.615	<u>0.7001</u>	<u>0.8906</u>	2.6354	3.1484	0.5739	0.7306	2.628	3.1355	1.2649	1.5934
Power	96	2143.0732	2856.9641	1836.5217	2529.4082	2764.0071	3575.76	<u>1670.7936</u>	<u>2303.7766</u>	2036.8491	2794.8821	1522.3687	2074.7476
	120	2242.8386	3000.8669	2104.397	2833.8071	2722.5266	3533.498	<u>1713.0022</u>	<u>2398.4294</u>	1838.0431	2528.269	1628.0834	2211.7373
	336	2186.8606	2932.5842	2596.7925	3343.2185	2636.1123	3439.8325	<u>1725.9772</u>	<u>2367.9302</u>	1790.873	2462.7583	1691.2375	2306.0332
	720	2186.1484	2932.2808	3843.0903	4912.8188	2705.8755	3507.7417	<u>1726.9525</u>	<u>2371.6135</u>	1929.9791	2648.4456	1687.792	2275.1616
Weather	96	15.115	76.1451	19.3862	83.9374	24.1458	95.8898	<u>16.9784</u>	<u>77.8039</u>	19.2918	86.6916	20.4612	85.7296
	120	14.2523	74.405	19.7799	83.9299	31.6785	115.1958	<u>17.1251</u>	<u>78.232</u>	18.9094	85.1188	22.0061	88.0541
	336	17.0746	80.4478	22.0616	88.0609	39.0595	123.9135	<u>19.0034</u>	<u>81.5563</u>	22.5815	101.2167	23.2499	91.4257
	720	17.2801	81.0746	23.0586	90.7269	33.3565	117.2401	<u>20.5038</u>	<u>84.5969</u>	22.9454	93.5754	22.2875	92.2548
IDEA	96	<u>3.4639</u>	<u>5.0895</u>	4.2096	6.0103	3.9454	6.0129	3.5394	5.3499	3.9759	5.6999	3.4133	5.0254
	120	4.1065	5.9336	4.2872	6.1407	4.045	6.0327	<u>3.7866</u>	<u>5.5256</u>	4.1262	5.9298	3.6312	5.2566
	336	5.3124	7.6573	5.198	7.6414	5.477	7.9939	<u>4.7302</u>	<u>7.209</u>	5.3044	7.6902	4.5895	6.9595
	720	5.786	8.5289	5.42	7.7834	6.0789	8.8711	<u>4.5095</u>	<u>6.7782</u>	6.3528	8.9245	4.123	6.1074
Electricity	96	22.3249	131.6917	23.1564	135.294	39.3555	230.2751	20.0137	117.3976	26.3083	159.4539	<u>21.253</u>	<u>123.2377</u>
	120	22.5418	136.1571	22.6835	132.0411	39.93	230.7552	19.7892	115.3996	25.833	153.0442	<u>20.3264</u>	<u>118.8906</u>
	336	25.658	149.9957	24.0349	140.3616	43.52	247.7342	19.8752	117.3849	29.3667	170.2018	<u>21.0625</u>	<u>122.6499</u>
	720	28.1319	161.8731	24.5551	142.4943	43.7687	250.6856	20.5075	120.3398	29.6541	170.4887	<u>21.9227</u>	<u>127.108</u>
ILINet	96	1.047	1.3825	0.9711	1.3406	1.0084	1.3843	0.8065	1.1873	1.0254	1.381	<u>0.822</u>	<u>1.1753</u>
	120	1.0305	1.3822	1.0636	1.4019	1.0225	1.3864	0.9111	1.2319	1.02	1.3859	0.7907	1.1895
	336	0.9805	1.372	1.0354	1.3867	1.011	1.3686	<u>0.8181</u>	<u>1.183</u>	0.9868	1.3694	0.7662	1.1439
	720	1.0201	1.4086	1.0084	1.3583	0.9916	1.3665	0.8341	1.1916	0.9879	1.389	<u>0.9548</u>	<u>1.3163</u>
ETTh1	96	1.0588	1.814	1.2783	2.1944	1.5711	2.7088	1.2677	2.1727	1.1626	2.044	<u>1.1193</u>	<u>1.8788</u>
	120	1.1217	1.9237	1.3056	2.246	1.5801	2.7297	1.2742	2.2063	1.2094	2.1281	<u>1.1567</u>	<u>1.942</u>
	336	<u>1.3016</u>	<u>2.2411</u>	1.4045	2.395	1.6982	2.8366	1.3316	2.2724	1.4021	2.4157	1.2983	2.2014
	720	1.3613	2.3575	1.4691	2.4962	1.8335	2.9676	1.3623	2.3265	1.5221	2.5617	<u>1.4266</u>	<u>2.4101</u>
ETTm1	96	<u>0.9104</u>	<u>1.5378</u>	1.0229	1.7308	1.5096	2.7256	0.9597	1.6596	0.9876	1.6513	0.8251	1.3728
	120	<u>0.9003</u>	<u>1.5249</u>	1.0444	1.7777	1.5809	2.7551	1.0035	1.7453	1.0261	1.7412	0.8597	1.4311
	336	<u>1.0347</u>	<u>1.779</u>	1.203	2.0774	1.7319	3.0085	1.1454	1.9641	1.2725	2.1953	1.0259	1.6978
	720	<u>1.1581</u>	<u>2.019</u>	1.3067	2.2297	1.8142	3.079	1.2016	2.0742	1.3998	2.4116	1.1518	1.9604
Total		13	13	1	1	0	0	22	22	0	0	27	27

Table 3: Forecasting Performance Comparison: ProbSparse vs top- K Sparse

Metric	Temperature		Power Consumption		IDEA		Weather		ILINet		Electricity		ETTh1		ETTm1	
	ProbSparse	top- k	ProbSparse	top- k	ProbSparse	top- k	ProbSparse	top- k	ProbSparse	top- k	ProbSparse	top- k	ProbSparse	top- k	ProbSparse	top- k
MAE	0.6072	0.6188	1528.6433	1505.6522	1.8723	1.4289	20.4503	20.3328	0.8099	0.8104	21.0915	0.0035	1.1471	1.1239	0.6587	0.6668
RMSE	0.7978	0.8094	2067.1826	2037.5034	2.5854	2.2710	37.0745	36.7800	1.1826	1.1735	28.0864	0.0044	1.5718	1.5430	0.9028	0.9170
R^2	0.9367	0.9349	0.9159	0.9183	0.9908	0.9925	0.7982	0.7977	0.2651	0.2764	0.8935	0.8864	0.8019	0.8099	0.9277	—

4.4 Training dynamics

To investigate the convergence of training loss of TWINFORMER we investigated training loss curves on all datasets. Here, in Figure 2, we present the training loss curves across four datasets only of TWINFORMER (blue) against a strong baseline of five models. In all cases, the TWINFORMER exhibits the fastest convergence and consistently reaches the lowest training loss by the end of training. It starts with a competitive and slightly higher loss in the first few epochs but quickly overtakes all baselines (Informer, FEDformer, iTransformer, PatchTST, and vanilla Transformer), maintaining a clear downward trajectory to achieve the best final performance on every dataset.

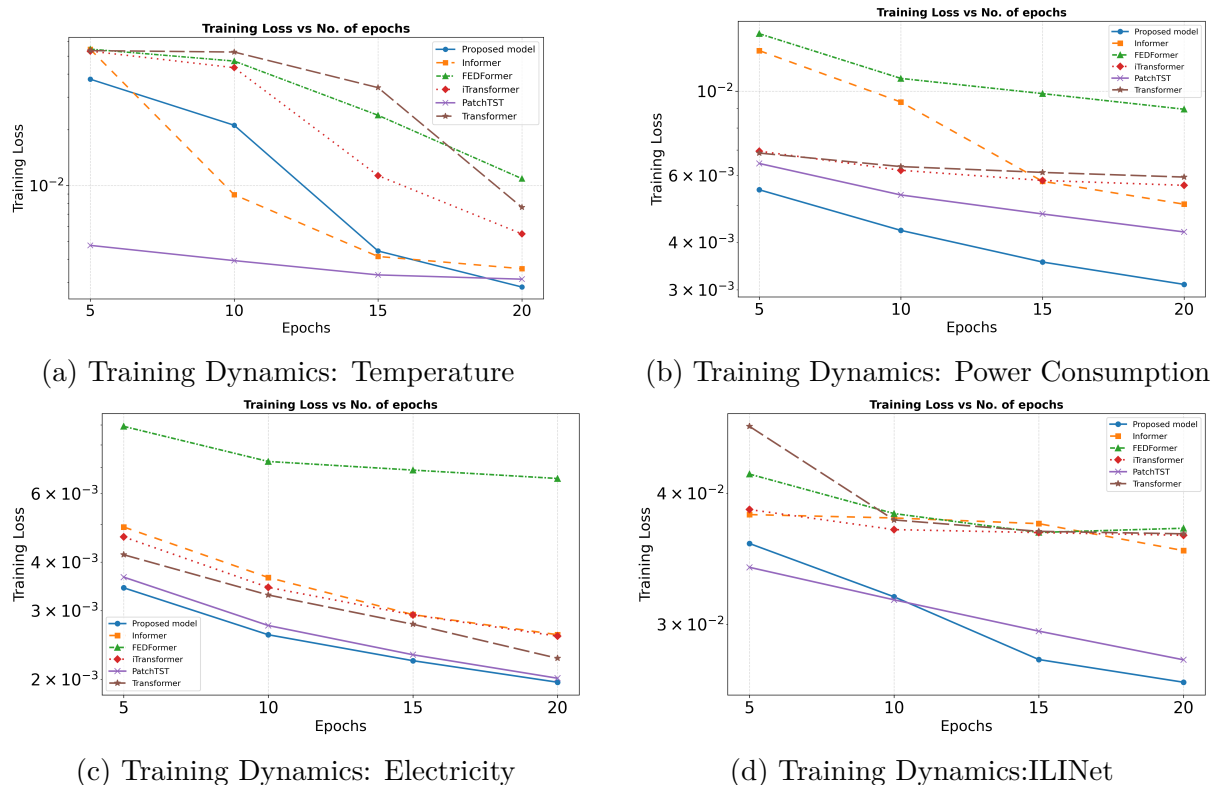


Figure 2: Training loss curves for TWINFORMER and five baselines over 20 epochs. The proposed model exhibits faster convergence and achieves the lowest final loss.

4.5 Ablation study

In this section, we present a comparison of forecasting performance between the baseline ProbSparse Attention mechanism and top- k Attention on all datasets. Our top- k model consistently outperforms and sometimes matches ProbSparse on the majority of datasets and evaluation horizons. Notably, it achieves substantial improvements in power consumption (MAE reduced from 1528.64 to 1505.65, RMSE reduced from 2067.18 to 2037.50), IDEA.NS (MAE 1.87 \rightarrow 1.43, RMSE 2.59 \rightarrow 2.27), and electricity (dramatic gains of several orders of magnitude in both MAE and RMSE, indicating significantly better capture of complex multivariate patterns). Competitive results are also observed on Weather, ETTh1, and ETTm1 datasets, while performance remains comparable on Temperature and ILINet. These results demonstrate that the proposed top- k selection strategy, directly identifies the most informative queries instead of relying on probabilistic

sparsity assumptions. It yields more effective attention patterns, leading to superior or equivalent predictive accuracy in long-sequence forecasting tasks.

We compared GRU with other sequence aggregators such as LSTM, Convolution 1D, and standard Attention-decoder for all datasets. In the Table 3, we are presenting only two datasets, namely, Temperature and Weather. On the univariate Temperature dataset, our GRU model achieves the best results across all three metrics, attaining an MAE of 0.6188, RMSE of 0.8094, and R^2 of 0.9349, outperforming LSTM by 3–4% relative improvement in error metrics and clearly surpassing both the convolutional and Attention-based decoders. On the more challenging multivariate Weather dataset, which contains 21 highly correlated meteorological variables, our GRU remains highly competitive, delivering an MAE of 20.3328 and an R^2 of 0.7977 and only marginally behind the best-performing baselines (Conv1D and Attention-Decoder for MAE and LSTM for RMSE and R^2), while maintaining robust and stable performance without the need for explicit Attention mechanisms. For other datasets, also GRU is giving the best MAE, RMSE and R^2 . These results highlight the reason to choose GRU in our model and making it a lightweight yet powerful baseline for time-series forecasting tasks across univariate and multivariate settings.

Table 4: Performance comparison across models for Univariate (Temperature) and Multivariate (Weather)

Dataset	Temperature				Weather			
Method	GRU	LSTM	Conv1D	Attn-Dec	GRU	LSTM	Conv1D	Attn-Dec
MAE	0.6188	0.6379	0.6977	2.5798	20.3328	20.1705	20.1558	19.7484
RMSE	0.8094	0.8293	0.9186	2.9376	36.7800	36.4578	36.9015	37.0422
R^2	0.9349	0.9316	0.9161	0.1421	0.7977	0.8061	0.8029	0.7960

5 Results and discussion

The experimental results shown in Table 2 demonstrate that the TWINFORMER outperforms other models across multiple datasets and prediction horizons. In the Temperature dataset, the proposed model achieved the lowest errors in three out of four horizons, outperforming baselines like PatchTST and iTransformer, particularly at shorter horizons (e.g., MAE of 0.5486 at 96 steps). For univariate datasets such as Power consumption and IDEA.NS, it consistently ranked first and for Temperature and ILINet data it performed best and second best MAE based on horizon. On the other hand the larger-scale multivariate datasets, such as Electricity, Weather, ETTh1, and ETTm1 TWINFORMER remains robust, ranking best for ETTm1 and often ranking second for others while staying close to the top performer (PatchTST). This suggests that the hierarchical local-to-global processing effectively handles both fine-grained local patterns and long-range inter-patch dependencies, even in high dimensional settings. The efficient performance of TWINFORMER can be attributed to key architecture validated in our experiment. The top- k sparse attention gives more stable and effective results than ProbSparse (Table 3), achieving consistent gains on Power Consumption, IDEA.NS, and Electricity datasets. The GRU-based sequence aggregator efficiently captures irreversible temporal dynamics across globally contextualized patches, outperforming alternatives like LSTM, Conv1D,

and Attention-decoder (Table 4). Faster convergence and lower final training loss (Figure 2) indicate that the hierarchical architecture enables more effective optimization compared to flat Transformer-based baselines.

Overall, the TWINFORMER secured the highest number of wins (here win is ranking in top two). Specifically, our model achieves 27 wins for both MAE and RMSE, in which we have 17 wins that are the best MAE and RMSE and 10 are the second best MAE and RMSE, surpassing PatchTST (22 wins in which 8 are the best MAE and RMSE, and 14 are the second best MAE and RMSE) and other models, indicating its robustness in multivariate time-series forecasting.

6 Conclusion

In this study, we introduced TWINFORMER, a hierarchical Transformer architecture that explicitly separates fine-grained intra-patch modelling from long-range inter-patch dependency capture, augmented by a lightweight GRU aggregator for direct multi-horizon forecasting. By combining fixed top- k Sparse Attention with a two-stage local-to-global processing pipeline inspired by successful vision hierarchies, TWINFORMER achieves state-of-the-art performance across eight diverse real-world datasets, outperforming strong contemporary baselines including PatchTST, iTransformer, FEDformer, Informer, and the vanilla Transformer.

The ablation studies further validate the design choices: replacing ProbSparse with top- k Attention provides consistent improvements and comparable performance across nearly all datasets, while the GRU-based sequence aggregator outperforms LSTM, Conv1D, and Attention-decoder alternatives, particularly on univariate and moderately multivariate series. The resulting architecture maintains linear memory and time complexity $O(kLd)$ with respect to input length L , enabling efficient training and inference on sequences exceeding 10^5 timesteps on a single consumer GPU.

Nevertheless, certain limitations remain. First, the use of top- k Sparse Attention, while improving computational efficiency, may inadvertently overlook important long-range dependencies that fall outside the selected Attention heads. Second, the current architecture employs a GRU-based decoder, which predicts all future time steps in a single forward pass. As a result, it cannot explicitly model temporal dependencies among the predicted future steps, which may limit its ability to capture fine-grained dynamics in highly stochastic and structured sequences.

References

- [1] I. Beltagy, M. E. Peters, and A. Cohan. Longformer: The long-document transformer. *arXiv preprint arXiv:2004.05150*, 2020.
- [2] G. E. P. Box, G. M. Jenkins, G. C. Reinsel, and G. M. Ljung. *Time Series Analysis: Forecasting and Control*. John Wiley & Sons, 5th edition, 2015.
- [3] P. Chen, Y. Zhang, Y. Cheng, Y. Shu, Y. Wang, Q. Wen, B. Yang, and C. Guo. Pathformer: Multi-scale transformers with adaptive pathways for time series forecasting. *arXiv preprint arXiv:2402.05956*, 2024.

- [4] R. Child, S. Gray, A. Radford, and I. Sutskever. Generating long sequences with sparse transformers. *arXiv preprint arXiv:1904.10509*, Apr. 2019.
- [5] K. Cho, B. van Merriënboer, C. Gulcehre, D. Bahdanau, F. Bougares, H. Schwenk, and Y. Bengio. Learning phrase representations using rnn encoder–decoder for statistical machine translation. In *Proceedings of the 2014 Conference on Empirical Methods in Natural Language Processing (EMNLP)*, pages 1724–1734, 2014.
- [6] A. Dosovitskiy, L. Beyer, A. Kolesnikov, D. Weissenborn, X. Zhai, T. Unterthiner, M. Dehghani, M. Minderer, G. Heigold, S. Gelly, J. Uszkoreit, and N. Houlsby. An image is worth 16x16 words: Transformers for image recognition at scale. *arXiv preprint:2010.11929*, 2020.
- [7] K. Han, A. Xiao, E. Wu, J. Guo, C. XU, and Y. Wang. Transformer in transformer. In M. Ranzato, A. Beygelzimer, Y. Dauphin, P. Liang, and J. W. Vaughan, editors, *Advances in Neural Information Processing Systems*, volume 34, pages 15908–15919. Curran Associates, Inc., 2021.
- [8] S. Hochreiter and J. Schmidhuber. Long short-term memory. *Neural computation*, 9(8):1735–1780, 1997.
- [9] D. P. Kingma and J. Ba. Adam: A method for stochastic optimization. *arXiv preprint arXiv:1412.6980*, 2014.
- [10] N. Kitaev, Ł. Kaiser, and A. Levskaya. Reformer: The efficient transformer. In *International Conference on Learning Representations (ICLR)*, 2020.
- [11] S. Lee, T. Park, and K. Lee. Learning to embed time series patches independently. *arXiv preprint arXiv:2312.16427*, Dec. 2023.
- [12] S. Li, X. Jin, Y. Xuan, X. Zhou, W. Li, Y. Zhuang, Q. He, and X. He. Enhancing the locality and breaking the memory bottleneck of transformer on time series forecasting. In *Advances in Neural Information Processing Systems (NeurIPS)*, 2019.
- [13] Y. Liu, T. Hu, H. Zhang, H. Wu, S. Wang, L. Ma, and M. Long. ITransformer: Inverted transformers are effective for time series forecasting. *arXiv*, Oct. 2023.
- [14] Z. Liu, J. Chen, and J. Tang. Time series forecasting with hierarchical attention. In *Proceedings of the International Joint Conference on Artificial Intelligence (IJCAI)*, 2022.
- [15] Y. Nie, Y. Yu, Q. Zhang, P. Gao, and Y. Zou. A time series is worth 64 words: Long-term forecasting with transformers. In *International Conference on Learning Representations (ICLR)*, 2023.
- [16] R. Pascanu, T. Mikolov, and Y. Bengio. On the difficulty of training recurrent neural networks. In S. Dasgupta and D. McAllester, editors, *Proceedings of the 30th International Conference on Machine Learning*, volume 28 of *Proceedings of Machine Learning Research*, pages 1310–1318, Atlanta, Georgia, USA, 2013. PMLR.
- [17] K. Rasul, C. Seward, T. Schmiedel, M. Lee, D. P. Kreil, and N. Pawłowski. Patchtst: Rethinking time series forecasting with transformers. *arXiv preprint arXiv:2205.13504*, 2022.

- [18] S. J. Taylor and B. Letham. Forecasting at scale. *Am. Stat.*, 72(1):37–45, Jan. 2018.
- [19] A. Vaswani, N. Shazeer, N. Parmar, J. Uszkoreit, L. Jones, A. N. Gomez, Ł. Kaiser, and I. Polosukhin. Attention is all you need. In *Advances in Neural Information Processing Systems (NeurIPS)*, volume 30, 2017.
- [20] S. Wang, B. Z. Li, M. Khabsa, H. Fang, and H. Ma. Linformer: Self-attention with linear complexity. In *Advances in Neural Information Processing Systems (NeurIPS)*, volume 33, 2020.
- [21] H. Wu, Y. Wang, X. Zhou, K. Huang, and H. Xiong. Autoformer: Decomposition transformers with auto-correlation for long-term series forecasting. In *Advances in Neural Information Processing Systems (NeurIPS)*, volume 34, pages 22419–22430, 2021.
- [22] Q. Wu, H. Zhou, X. Wu, H. Sun, J. Peng, J. Li, and H. Xiong. Timesnet: Temporal 2d-variation modeling for general time series analysis. In *International Conference on Learning Representations (ICLR)*, 2023.
- [23] H. Zhou, J. Peng, S. Zhang, J. Li, H. Xiong, and W. Zhang. Fedformer: Frequency enhanced decomposed transformer for long-term series forecasting. In *International Conference on Machine Learning (ICML)*, 2022.
- [24] H. Zhou, S. Zhang, J. Peng, S. Zhang, J. Li, Y. Xiong, and S. Sundaram. Informer: Beyond efficient transformer for long sequence time-series forecasting. In *Proceedings of the AAAI Conference on Artificial Intelligence*, volume 35, pages 11106–11115, 2021.

7 Appendix

In Table 5, we have predicted a 5-day horizon for all datasets. We did experiments on seven datasets, in which for three datasets we got the best MAE and RMSE; for the Power consumption dataset we got the second-best MAE but the best RMSE. For other datasets also we are getting competing results. Overall, these results provide the robustness and effectiveness of the TWINFORMER handling of short time horizon forecasting also compared to other state-of-the-art models.

Table 5: Forecasting performance across datasets and models for a five-day horizon

Model	Temperature		Power Consumption		IDEA.NSstock		Weather		ILINet		Electricity Load		ETTh1	
	MAE	RMSE	MAE	RMSE	MAE	RMSE	MAE	RMSE	MAE	RMSE	MAE	RMSE	MAE	RMSE
TWINFORMER	0.5711	0.7483	<u>1152.40</u>	1537.41	1.0494	1.8526	14.1749	76.0811	0.6092	1.0439	17.1841	104.3144	1.2498	1.6386
Informer	0.7512	0.9470	1116.20	<u>1595.80</u>	3.0952	4.5070	14.3880	44.2848	1.1034	1.7452	20.3671	121.6163	<u>1.2015</u>	<u>1.5923</u>
FEDFormer	0.7791	0.9987	1965.22	2570.31	2.1332	3.4599	11.7195	38.4354	1.0618	1.7185	24.0549	141.5632	1.2514	1.7056
PatchTST	0.5346	0.7008	1706.46	2262.92	<u>1.4921</u>	<u>2.2674</u>	15.3620	44.7890	1.1221	1.6005	18.3520	109.2451	1.0469	1.4345
iTransformer	0.6940	0.8888	1990.32	2648.48	2.6450	4.0946	<u>13.5195</u>	<u>77.1390</u>	1.0136	1.5471	18.0912	108.6458	1.3347	1.7641
Vanilla Transformer	<u>0.5465</u>	0.7174	1879.07	2483.94	2.0553	3.2613	17.0264	53.2474	<u>0.9509</u>	<u>1.5379</u>	<u>17.6341</u>	<u>109.5644</u>	1.2863	1.6791